Unsteady flow analysis of hinged and sliding door openings

Fredrik Kihlberg*, Øystein Formo Hermansen, Arnab Chaudhuri

Department of Civil Engineering and Energy Technology
OsloMet – Oslo Metropolitan University, Oslo, Norway
**fre.kihlberg@gmail.com*

Abstract

Existing thermal condition and indoor air quality have a big impact on our work performance, comfort, and health in an indoor environment. Apart from many other parameters, door motions and human movements play crucial role in mass and thermal exchange affecting safety and/or energy management issues in various situations. An isolation room in a hospital setup, for instance, helps to protect patients and staff against the risk of infection by airborne pathogens. Another example is cold storage room facilities, where temperature and moisture control are the key parameters for an optimal operation and energy usage. In this study, we present a transient flow analysis of door motions in indoor environment. The flow physics is resolved by solving 3D compressible RANS (Reynolds-averaged Navier-Stokes) equations together with the energy and species transport equations and two-equation turbulence models utilizing an overset mesh strategy to address the rigid body motion of doors in a relevant fluid domain involving air and sulfur hexafluoride (SF_6). Simulations are performed for three different types of doors, namely a hinged door, a two-way sliding door, and a sliding door considering door opening and closing phases. Transient flow-field data through the door opening area have been processed and a comparative analysis is performed considering the mass flux of the constituents, normal velocity, cumulative mass exchange through the different doors.

1. Introduction

We spend the majority of the time in indoor environment and our work performance, comfort and health are heavily impacted by the indoor temperature and air quality. In certain special environments, such as hospital isolation rooms and clean rooms, it is particularly important to understand the process of pollutant transmission. In healthcare settings, isolation rooms are used to contain infectious patients or to protect vulnerable patients from infection. On the other hand, in cold storage room facilities, for instance, the temperature and moisture control are the key parameters for an optimal operation and energy usage. These are widely applicable for industries like food, pharmaceutical, photographic and more. Multiple coupled interactions, involving heat-mass-momentum transfer and phase change of constituent components play important roles during the operating condition of a cold storage room in such applications. Among several other factors, infiltration of hot and moist air through open doors become crucial for the infiltration load and the performance of buildings. Often, a big difference in temperature exists between the adjacent rooms and this may alter due to the door opening. In these scenarios, understanding of air flow, mass/heat exchange by the opening of a door is beneficial for control strategies. The effect of door motion is not only relevant for special rooms. It is also very relevant for example in educational and office buildings. It can be realized that the analysis of the combined effect of human motion along with and the door openings are necessary often for predicting realistic situations. In their study, Tang et al. [1] emphasized that there is likely to be some leakage across the doorway to a lesser or greater degree as a human moves through the door at a reasonable walking speed affecting the flow physics. Shao et al. [2] and Kalliomäki et al. [3] have drawn similar conclusions in their experimental work. In the following paragraph, we provide a brief account of both experimental and numerical studies of the literature regarding this field.

Several studies show that door opening motion generates a notable air exchange and airborne contaminant transfer across a doorway. This effect is especially notable for a hinged door [1, 3–6]. Also, the effect is larger when a person passes through a doorway. The amount of contaminant transfer is influenced by door hold open time and temperature difference. Tang et al. [7] investigated a clinical situation where a severe case of adult chickenpox was managed in a negative pressure isolation room, with no adjacent anteroom. Previous studies have also shown that the hinged doors allow more mass exchange than sliding doors. In the similar context, Eames et al. [8] have estimated motion and diffusion of a contaminant in an isolation room, in the absence of differential pressure. Several authors performed experimental studies, often with smoke as tracer fluid or particle generators to simulate transmission, e.g. small scale model of adjacent rooms [9], connected rooms [10], clean room with double hinged door [2]. In this regard, Hathway et al. [11] performed a field and small scale study of rooms with hinged type doors in office and hospital settings. They have used water as the tracer fluid in their small scale model showing that there exists a linear relationship between time doors are held open and air volume flux. On the other hand, the experimental works presented in [3, 12–14] considered full scale models and realistic setups. In the context of

the recent pandemic situation, Bhattacharya et al. [15] investigated positively pressurized room with a physical model. The goal of their study was to examine the possibility of the COVID19 virus, contaminating clean areas due to the door opening and closing motion. Apart from experimental approach, Computational fluid dynamics (CFD) simulations are widely used to resolve detailed, complex flow dynamics associated with the indoor environment. Numerical approach via CFD solutions are increasingly used nowadays in design, optimization of ventilation systems, and the prediction of air movement in ventilated spaces. Several studies [4, 16–22] reported CFD analysis of the effect of the door motion in various scenarios. Among these [18, 19, 22] analyzed cold storage facilities and Zhang et al. [21] studied refrigerated vehicles via numerical approach. Note that the experimental work of Tang et al. [1] revealed that sliding doors (single or double) are advantages over the more conventional hinged-door towards general infection control purposes. However, systemic numerical studies addressing a comparison of different type of door motions are not abundant.

In this work, we revisit and explore the effect of door opening motion considering three different types of door by numerical approach. To address this, we solve 3D compressible RANS equations together with the energy and species transport equations and two-equation turbulence models are used to account the effects of turbulence. An overset mesh strategy is utilized to resolve the rigid body motion of doors in a relevant fluid domain involving air and SF_6 as working fluids. The article is organized as follows. First, we present the governing equations and numerical setup for the different cases in section 2. The description of the problem setup is provided in section 3, followed by results and discussions in section 4. Finally, the conclusions are drawn in section 5.

2. Method

2.1. Governing equations

The multi-component gas system consisting of air and SF_6 is governed by 3D compressible Navier-Stokes system of equations together with mass, species conservation and energy conservation equations. For any conserved property ($\rho\phi$), the general transport equation can be expressed as in the following standard notation [23]:

$$\frac{\partial \rho\phi}{\partial t} + \vec{\nabla} \cdot \rho\phi\vec{V} = \vec{\nabla} \cdot \Gamma\vec{\nabla}\phi + S_\phi, \tag{1}$$

where ρ is the density, $\vec{V}$ is the velocity and Γ is the diffusion coefficient. The first and second terms in the left hand side are known as the temporal term and the advection term respectively. The right hand side consists of the diffusion term and the generation term (S_ϕ). We solve the unsteady Reynolds averaged Navier-Stokes (RANS) formulation and Realizable $\kappa - \epsilon$ model is used for turbulence. The multi-component gas mixture is assumed to be Newtonian fluid and follow ideal gas law. The finite volume method (FVM) based commercial CFD tool StarCCM+ is used to perform the simulations. An overset mesh strategy is employed to address the rigid body motion of the doors in the fluid domain. A background mesh (throughout the computational domain) and overset mesh (section of domain, including door and a surrounding region of choice) are generated for this purpose. The time varying rigid body rotation/translation motion is applied according to the desired door motion by setting the motion parameters associated with the door geometry. The overall setup of the different test cases is described in section 3. The brief description of the numerical schemes used in the present study is as follows. Second order upwind schemes for convection, hybrid Gauss least-squared gradient method based 2nd order schemes for diffusion and Venkatakrishnan limiter function are chosen in solver setup. Second order implicit scheme (Newmark method) is used for time integration with a time step $\Delta t = 0.005\,\mathrm{s}$. Algebraic Multi-Grid (AMG) techniques are also invoked with the setup mentioned above. In Star-CCM+, under physics continua, the following models were chosen: coupled energy, coupled flow, coupled species, gradients, ideal gas, implicit unsteady, k-epsilon turbulence, multi-component gas (with air and SF6 as gas components), non-reacting, overset conservation, realizable k-epsilon two-layer, Reynolds-averaged Navier-Stokes, solution interpolation, three dimensional, turbulent, two-layer all y+ wall treatment, and wall distance. Standard values were used for all of these, excluding multi-component gas composition. The gas mixture composition is assigned as desired and is given in section 3.

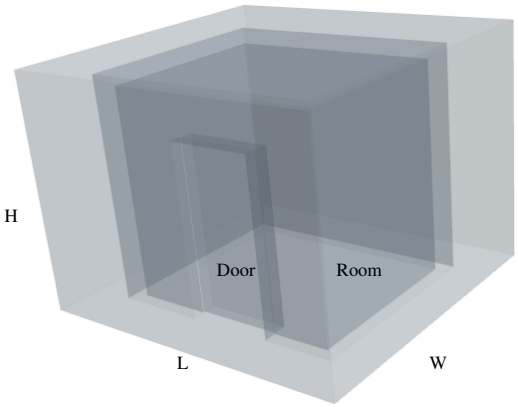

Figure 1: 3D view of the computational domain.

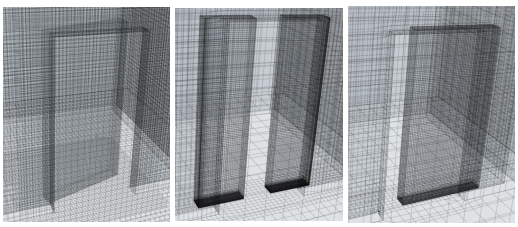

(a) hinged (b) two-way sliding (c) sliding

Figure 2: Partially opened doors.

Table 1: Dimensions of the model

	W (m)	L (m)	H (m)
Boundary	3.60	3.80	2.75
Outer wall	2.405	2.85	2.6
Inner wall	2.105	2.55	2.45
Two-way sliding door	0.15	0.5	1.98
Single door	0.15	1.00	1.98

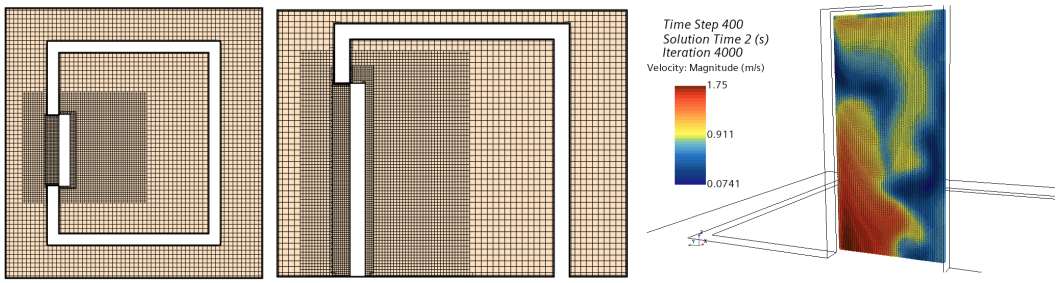

Figure 3: left: mid x-y plane (top view), middle: mid x-z plane (side view), right: presentation grid (y-z plane) at t = 2.0s

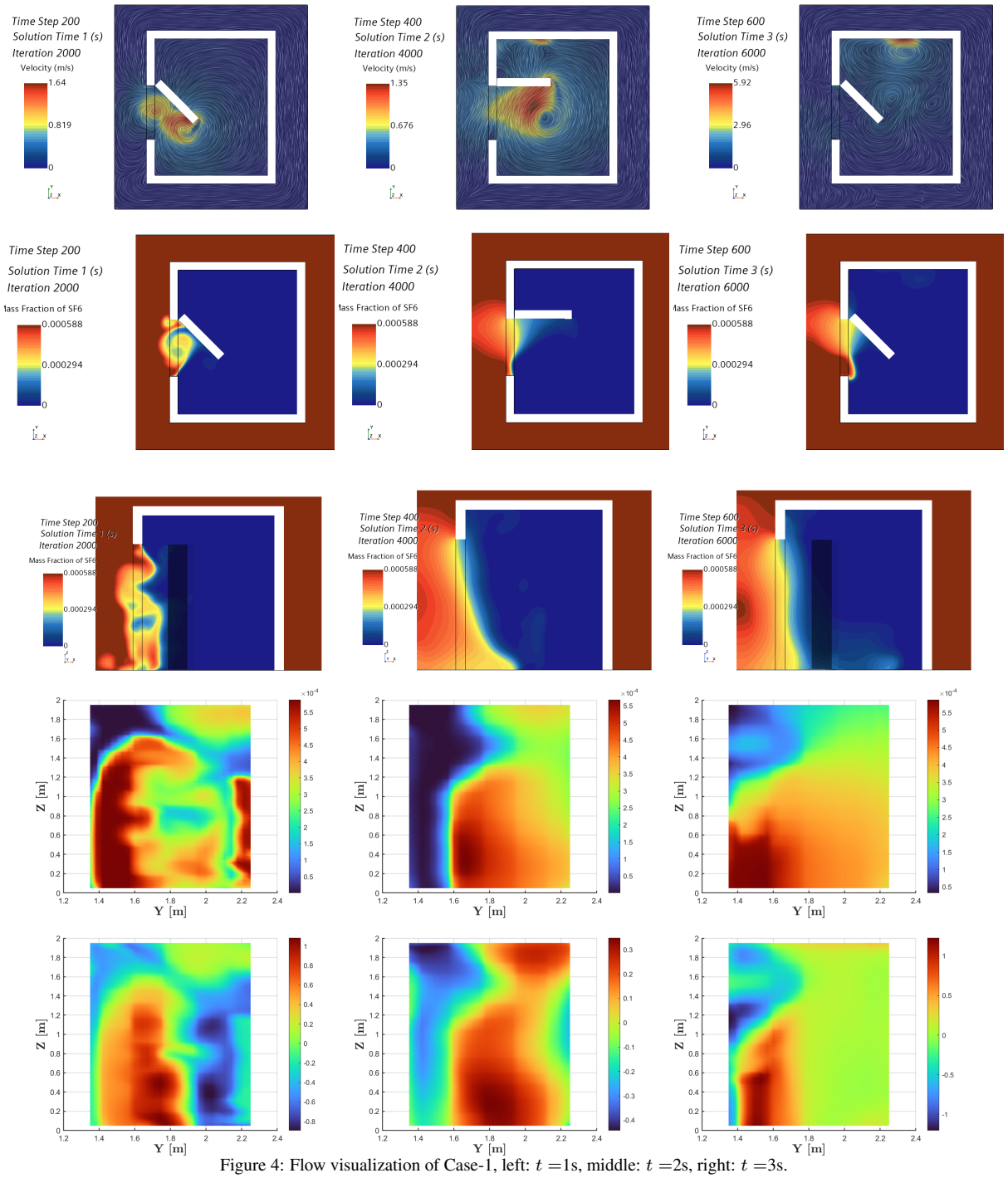

Figure 4: Flow visualization of Case-1, left: t =1s, middle: t =2s, right: t =3s.

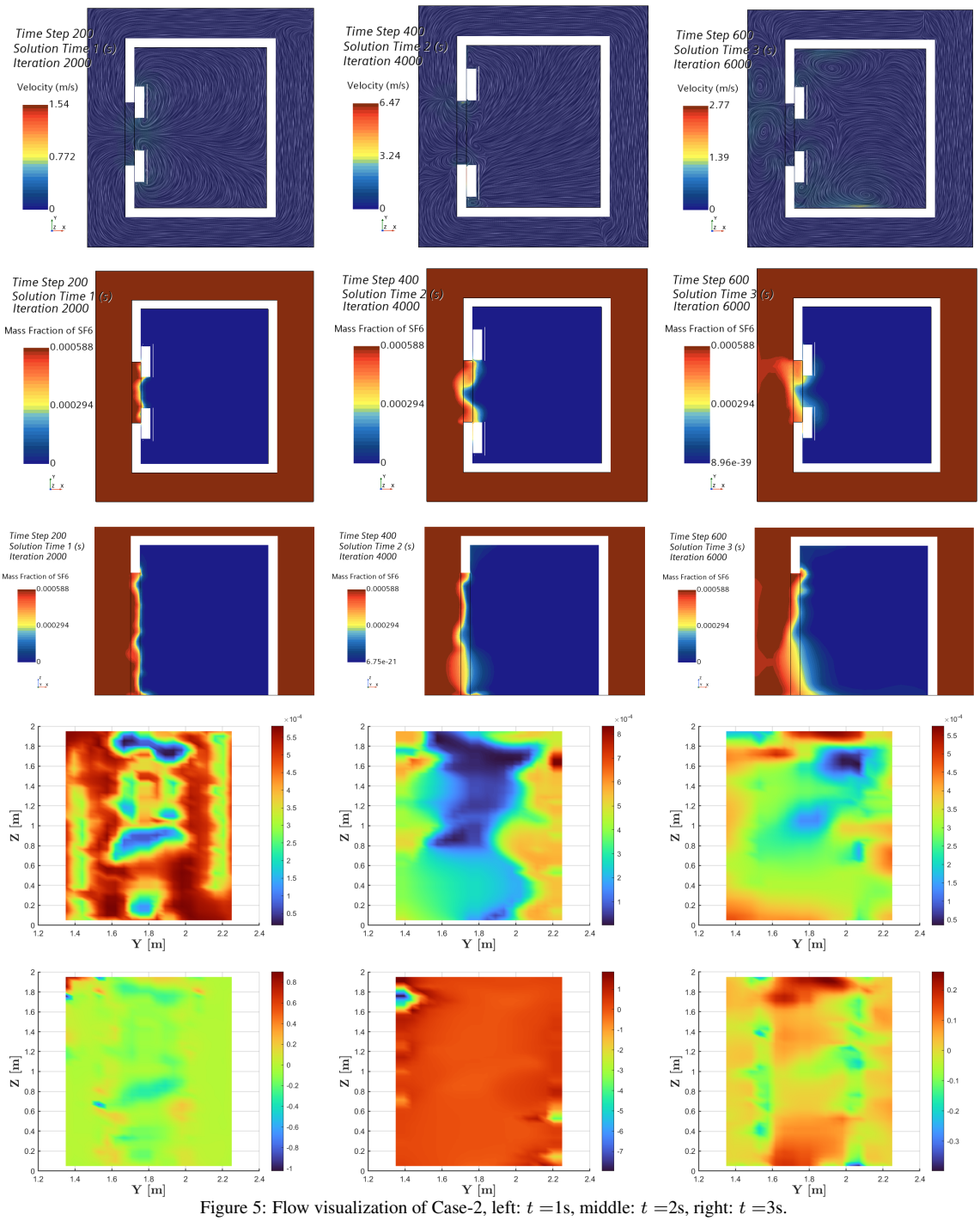

Figure 5: Flow visualization of Case-2, left: t =1s, middle: t =2s, right: t =3s.

3. Problem setup

A room with a door and a simplified connected outer corridor type area is made as computational domain (see the schematic in figure 1). Table 1 summarizes the Length (L), Width (W) and Height (H) of different components of the computational domain. All walls of the room are considered adiabatic. The initial condition of the fluid domain is set as: temperature, $T = 300$K, velocity field $\vec{V} = 0$, pressure $P = 101325$Pa, turbulent kinetic energy $k = 1.0e^{-3}$ J/kg and turbulent dissipation rate $\epsilon = 1.0e^{-6}$ m^2/s^3. The mass fraction of the SF_6 in the outer region is set as $Y_{SF6} = 0.00058$. This corresponds to the concentration of SF_6 to be 706.2 mg/m3. The room is considered as filled with pure air and devoid of any SF_6 at the initial state. The initial condition of mass fraction of SF_6 is similar to that reported by Chang et al. [4].

In this work, we consider three different type of doors, namely hinged, two-way sliding (also known as double sliding) and sliding. Figure 2 shows orientation of the partially opened doors for all three cases. The door

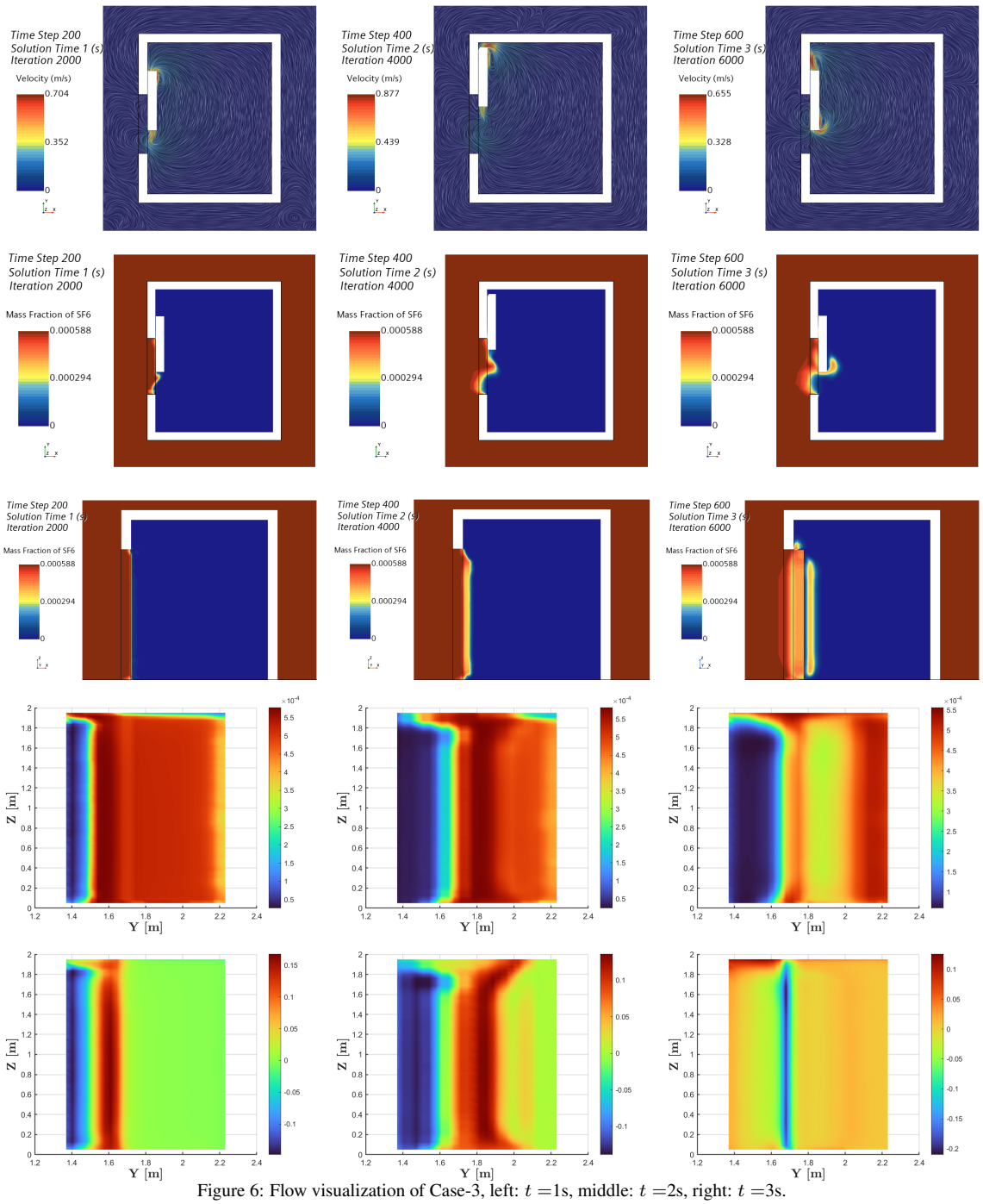

Figure 6: Flow visualization of Case-3, left: t =1s, middle: t =2s, right: t =3s.

opening-closing motions are assigned to different types of doors as follows. For hinged door, we set the opening with -0.785 radian/s during $0 < t \leq 2$s and closing with +0.785 radian/s when $2\text{s} < t \leq 4$s. In case of the two-way sliding door, the opening is set to ± 0.25 m/s during the initial 2s and the closing is set for next 2s with $\mp$ 0.25 m/s. Similarly, the door motion of sliding door is set as opening with +0.5 m/s during initial 2s and closing with -0.5 m/s when $2\text{s} < t \leq 4$s. Suitable user defined field functions are assigned to apply these door motions and to set initial mass fraction distribution in the computational domain. Simulations are executed till the final physical time reaches 4 second for all cases.

The mesh for the simulations consists of a background mesh and an overset mesh around the moving door. Additionally, we use refined mesh near the entrance of the door to resolve the flow physics. Note that the refinement zone varies depending upon the type of the door. The background mesh size was set to 20cm, the overset mesh size was set to 2cm, and the refinement mesh size was set to 4cm. The background mesh and the overset mesh region had two prism layers, while the refinement mesh region had five prism layers. For this, we have used the "Trimmer" mesh model of StarCCM+. Figure 3 illustrates the mesh setup for the hinged type door. The total number of cells (background cells together

with the cells in the overset region) are 673221, 400539, and 529740 for hinged door, sliding door and two-way sliding door respectively. A suitable "derived part" called presentation grid is generated at the location of door to record time varying solution data and analyze the mass exchange through the door opening. This is shown in figure 3 as an example with hinged door. The presentation grid contains 20×40 data points for post processing giving a resolution of $\Delta y = \Delta z \approx 0.05$m.

4. Results and discussions

We define Case-1 as hinged door, Case-2 as two-way sliding door and Case-3 as sliding door henceforward. We will present the results of each case with line integral convolution (LIC) of $\vec{V}$ and contour plots of other field variables mainly in three different planes. As shown in figure 3, these are the mid x-y plane (top view), mid x-z plane (side view) and presentation grid (y-z plane). Figures 4, 5 and 6 are for Case-1, Case-2 and Case-3 respectively. Note that these plots are presented systemically as follows: topmost row with LIC of $\vec{V}$ (top view), second row from the top with Y_{SF6} (top view), third row from the top with contours of Y_{SF6} (side view), second row from the bottom with contours Y_{SF6} (presentation grid i.e., door frame) and bottom row with contours of u-component of $\vec{V}$ (presentation grid i.e., door frame).

4.1. Flow evolution and general characteristics for different types of doors

The time evolution of door opening and closing for Case-1 is depicted in figure 4. First, it can be clearly seen from the LIC of $\vec{V}$ that quite large vortex structures exist during the flow evolution. The hinged door makes and angle of $\approx 45^\circ$ at 1s during the opening phase, $\approx 90^\circ$ fully open at 2s and in the closing phases at 3s it again makes an angle of $\approx 45^\circ$. The complex, highly three dimensional shear/mixing layers are clearly seen from the distribution of mass fraction of SF_6 in x-y, x-z and y-z planes revealing a substantial extent of mixing of SF_6 from outside into the room. The u-component of the velocity field is normal to the door opening plane. Note that a positive u-component is associated with the normal velocity field that is entering to the room. On the other hand, a negative u-component is associated with the normal velocity field that is leaving the room. The contours of u-component match well with the contours of Y_{SF6}.

Figure 5 illustrates the flow development of Case-2. Note that, similar to the hinged door, two-way sliding door completely opens at 2s and closes at 4s. The door remains approximately half open at 1s and 3s during the opening phase and during the closing phase respectively. Noticeably, the vortex structures are entirely different than a hinged door. Also, it is clear that the penetration of mixing due the door induced movements are relatively less in this case compared to Case-1. Nevertheless, the contours of Y_{SF6} and u-component of the $\vec{V}$ at the door frame reveal the existing complex three dimensional nature of the mixing process. One could realize that the shear-layer instability induced by the door motion in Case-2 is different than Case-1.

The results for Case-3 are depicted in figure 6. Note that, due to the existing dimension of the room the sliding door is not completely open ($\approx$ 80% open). The mixing behavior shows some two-dimensional nature in the middle region of the door opening. These can be seen from the contour structures of Y_{SF6} and u-component of the velocity (see y-z planes). The three dimensional nature is visible in the upper and lower parts of the door opening area. This corroborates the mixing layer behavior visible at x-y plane (second row from the top of the figure 6). The contours of u-component of the velocity (positive and negative patches) are in accordance with the contours of Y_{SF6}.

4.2. Quantitative comparison of different doors

In order to quantify the mass of SF_6 exchanged through the door opening area one need to estimate first the surface averaged flow rate of SF_6,

$$\dot{M}_{\text{SF6}} = \iint_A (\rho Y_{\text{SF6}}\, \vec{V} \cdot \vec{n}\, dA) \tag{2}$$

where the A represent the door opening area. The instantaneous mass of SF_6 exchanged can thus be calculated by $M_{\text{SF6}}(t) = \dot{M}_{\text{SF6}}\, dt$. The transient data stored via presentation grid mentioned before is used to compute this. We compare $M_{\text{SF6}}(t)$ and the cumulative exchange of mass of SF_6 exchanged through the door opening for all cases. Figure 7 shows the instantaneous exchange of mass of SF_6 through the door opening for each case. The comparison of the cumulative exchange of mass of SF_6 through the door opening is presented in figure 8.

Table 2: Comparison of mass exchange at $t = 4$ s.

	Cumulative mass of SF_6 exchanged (kg)
Case-1	$\approx 1.30e^{-4}$
Case-2	$\approx 2.79e^{-5}$
Case-3	$\approx 2.87e^{-5}$

It can be seen from figure 7a that during the door opening phase of Case-1, the mass of SF_6 through the door remains mostly positive meaning the net influx into the room. On the other hand, during the closing phase of 2s to 4s the mass exchange changes sign after $\approx$3.5s. This passes through an oscillatory behavior around 2.7-2.8s. In figure 8a, the cumulative exchange of mass of SF_6 reflects these behaviors. The opening phase of the door opening shows almost linear growth, and a local saturation of the mass exchange occurs between 2-3s. The cumulative mass exchange drops to $1.30e^{-4}$ kg at 4s after a global maximum of $\approx 1.52e^{-4}$ kg. Case-2 and Case-3 show local spikes at the instance of change the door motion from opening to closing direction. Similar spikes (not shown for brevity) are observed of the average u-component of the velocity field through the doors at those instances for Case-2 (0.51 m/s) and Case-3 (-0.044 m/s) accordingly. Our preliminary mesh dependency study considering 4cm, 3cm and 2cm refined mesh sizes in the door interaction zone reproduces this behavior for Case-3. However, note that a detailed mesh sensitivity analysis is not performed taking the complete computational domain. Nevertheless, the behavior of the instantaneous mass exchange of Case-2 is different than Case-3. During the door opening phase, we found a relatively smooth non-linear growth in the cumulative mass exchange for Case-3. At the final stage (4s), the values for both Case-2 and

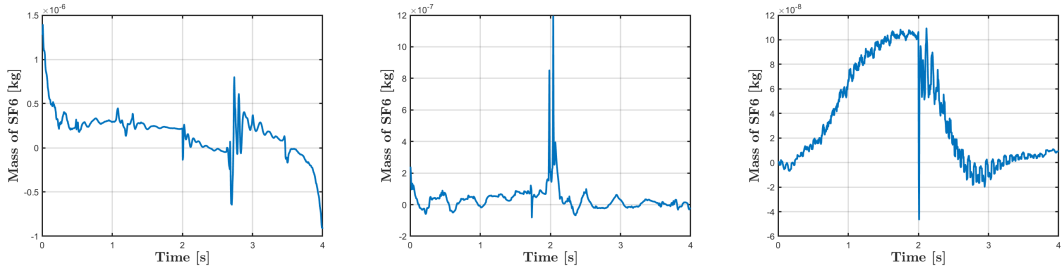

(a) hinged door (b) two-way sliding door (c) sliding door

Figure 7: Comparison of instantaneous exchange of the mass of SF6.

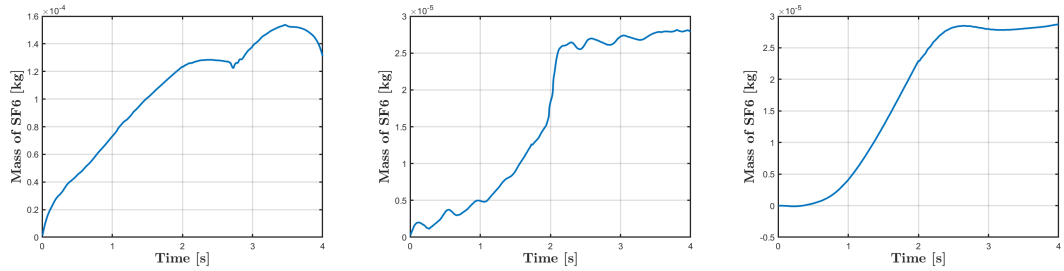

(a) hinged door (b) two-way sliding door (c) sliding door

Figure 8: Comparison of cumulative exchange of mass of SF_6.

case-3 yielded comparable magnitudes. However, these are an order of magnitude lower than Case-1. Table 2 summarizes the cumulative mass exchange of SF_6 through the different doors. Table 3 shows the CPUh required for each simulation.

Table 3: Computing time

	Central Processing Unit hours (CPUh)
Case-1	≈ 145
Case-2	≈ 66
Case-3	≈ 68

5. Conclusions

In this study, we presented a systematic analysis of mass exchange through the door opening and closing scenarios for three different types of doors. The complex unsteady flow physics involves multi-component gaseous system with rigid body motion of the doors. We solved 3D compressible RANS equations together with the energy and species transport equations. The effects of turbulence are resolved by two-equation turbulence models. An overset mesh strategy is employed to address the rigid body motion of doors in a relevant fluid domain consisting of air and SF_6 s working fluids. Simulations are made until the physical time reaches 4 second. The initial 2s is meant for door opening while door closing phase is performed during the last 2s. The detailed flow dynamics of each test cases have been illustrated with the contours of flow-field variable. The preliminary findings of the comparison reveal that under the similar condition the overall cumulative exchange of mass is SF_6 is about an order of magnitude less for both two-way sliding door and sliding door when compared with hinged door (≈ 4.6 times less). Matching with previous findings the case with hinged door is found be associated with most complex 3D mixing layers with maximum mass exchange. With the present setup, we observed similar mass exchange for two-way sliding and sliding door.

The authors would like to emphasise that the present study lacks comparison and validation of these preliminary findings with experimental data. We will consider the limitations of the present study in our subsequent work. The future work will also consider systematic numerical analysis of thermal effects, ventilation strategies, human motion in realistic indoor environment with different scenarios, different door and room size ratios.

Acknowledgment

This work is compiled and expanded from a part of the Master thesis work of the first author. The authors greatly acknowledge the commercial computer program StarCCM+, used in this study. The results are obtained by the licensed version 2022.1 17.02.007 of StarCCM+. The work utilized standalone Windows machines as well as the super-computing facility of Fram computer cluster (UiT Arctic University of Norway) under the project NN8005K at Notur, UNINETT Sigma2 AS (National infrastructure for scientific computational science in Norway).

References

[1] J. W. Tang, A. Nicolle, J. Pantelic, C. A. Klettner, R. Su, P. Kalliomaki, P. Saarinen, H. Koskela, K. Reijula, P. Mustakallio, D. K W Cheong, C. Sekhar, and K. Wai Tham, "Different types of door-opening motions as contributing factors to containment failures in hospital isolation rooms," *PloS One*, vol. 8, no. 6, p. e66663, 2013.

[2] X. Shao, K. Hashimoto, L. Fang, A. K. Melikov, K. G. Naydenov, and C. Rasmuseen, "Experimental study of airborne particle transmission through the doorway of a cleanroom due to the movement of a person," *Building and Environment*, vol. 183, p. 107205, 2020.

[3] P. Kalliomäki, P. Saarinen, J. W. Tang, and H. Koskela, "Airflow patterns through single hinged and sliding doors

in hospital isolation rooms – effect of ventilation, flow differential and passage," *Building and Environment*, vol. 107, pp. 154–168, 2016.

[4] L. Chang, X. Zhang, S. Wang, and J. Gao, "Control room contaminant inleakage produced by door opening and closing: Dynamic simulation and experiments," *Building and Environment*, vol. 98, pp. 11–20, 2016.

[5] I. G. Papakonstantis, E. A. Hathway, and W. Brevis, "An experimental study of the flow induced by the motion of a hinged door separating two rooms," *Building and Environment*, vol. 131, pp. 220–230, 2018.

[6] P. Kalliomäki, P. Saarinen, J. W. Tang, and H. Koskela, "Airflow patterns through single hinged and sliding doors in hospital isolation rooms," *International Journal of Ventilation*, vol. 14, no. 2, pp. 111–126, 2015.

[7] J. W. Tang, I. Eames, Y. Li, Y. Taha, P. Wilson, G. Bellingan, K. Ward, and J. Breuer, "Door-opening motion can potentially lead to a transient breakdown in negative-pressure isolation conditions: the importance of vorticity and buoyancy airflows," *Journal of Hospital Infection*, vol. 61, no. 4, pp. 283–286, 2005.

[8] I. Eames, D. Shoaib, C. Klettner, and V. Taban, "Movement of airborne contaminants in a hospital isolation room," *Journal of the Royal Society Interface*, vol. 6, no. suppl_6, pp. S757–S766, 2009.

[9] L. Fontana and A. Quintino, "Experimental analysis of the transport of airborne contaminants between adjacent rooms at different pressure due to the door opening," *Building and Environment*, vol. 81, pp. 81–91, 2014.

[10] J. Hendiger, M. Chludzińska, and P. Zietek, "Influence of the pressure difference and door swing on heavy contaminants migration between rooms," *PloS One*, vol. 11, no. 5, pp. e0 155 159–e0 155 159, 2016.

[11] A. Hathway, I. Papakonstantis, A. Bruce-Konuah, and W. Brevis, "Experimental and modelling investigations of air exchange and infection transfer due to hinged-door motion in office and hospital settings," *The International Journal of Ventilation*, vol. 14, no. 2, pp. 127–140, 2015.

[12] P. Kalliomäki, K. Hagström, H. Itkonen, I. Grönvall, and H. Koskela, "Effectiveness of directional airflow in reducing containment failures in hospital isolation rooms generated by door opening," *Building and Environment*, vol. 158, pp. 83–93, 2019.

[13] E. S. Mousavi, R. Jafarifiroozabadi, S. Bayramzadeh, A. Joseph, and D. San, "An observational study of door motion in operating rooms," *Building and Environment*, vol. 144, pp. 502–507, 2018.

[14] A. Bhattacharya, A. R. Metcalf, A. M. Nafchi, and E. S. Mousavi, "Particle dispersion in a cleanroom - effects of pressurization, door opening and traffic flow," *Building Research and Information: The International Journal of Research, Development and Demonstration*, vol. 49, no. 3, pp. 294–307, 2021.

[15] A. Bhattacharya, A. Ghahramani, and E. Mousavi, "The effect of door opening on air-mixing in a positively pressurized room: Implications for operating room air management during the covid outbreak," *Journal of Building Engineering*, vol. 44, p. 102900, 2021.

[16] L. Wang, L. Zhang, and G. Lian, "A cfd simulation of 3d air flow and temperature variation in refrigeration cabinet," *Procedia Engineering*, vol. 102, pp. 1599–1611, 2015.

[17] S. Lee, B. Park, and T. Kurabuchi, "Numerical evaluation of influence of door opening on interzonal air exchange," *Building and Environment*, vol. 102, pp. 230–242, 2016.

[18] J. Gonçalves, J. Costa, and A. Lopes, "Analysis of the air infiltration through the doorway of a refrigerated room using different approaches," *Applied Thermal Engineering*, vol. 159, p. 113927, 2019.

[19] S. Tian, Y. Gao, S. Shao, H. Xu, and C. Tian, "Numerical investigation on the buoyancy-driven infiltration airflow through the opening of the cold store," *Applied Thermal Engineering*, vol. 121, pp. 701–711, 2017.

[20] B. Zhou, L. Ding, F. Li, K. Xue, P. V. Nielsen, and Y. Xu, "Influence of opening and closing process of sliding door on interface airflow characteristic in operating room," *Building and Environment*, vol. 144, pp. 459–473, 2018.

[21] X. Zhang, J. Han, J. Qian, Y. Wang, L. Wang, and X. Yang, "Computational fluid dynamic study of thermal effects of open doors of refrigerated vehicles," *Journal of Food Process Engineering*, vol. 41, no. 3, pp. e12 662–n/a, 2018.

[22] A. Ayarmal, O. Melhus, and A. Chaudhuri, "The effects of fan and door opening on a cold storage room: a numerical study," *Linköping Electronic Conference Proceedings*, 2018.

[23] H. K. Versteeg and W. Malalasekera, *An introduction to computational fluid dynamics: the finite volume method*. Pearson Education, 2007.